Title

The Effects of Interlocking a Universal Hip Cementless Stem on Implant Subsidence and Mechanical Properties of Cadaveric Canine Femora

Journal

Veterinary Surgery, 45(2)

ISSN

0161-3499

Authors

Buks, Yonathan
Wendelburg, Kirk L
Stover, Susan M
et al.

Publication Date

2016-02-01

DOI

10.1111/vsu.12437

Peer reviewed

The Effects of Interlocking a Universal Hip Cementless Stem on Implant Subsidence and Mechanical Properties of Cadaveric Canine Femora

Yonathan Buks[1], Kirk L. Wendelburg[1], Susan M. Stover[2], and Tanya C. Garcia-Nolen[2]

[1]Animal Specialty Group, Los Angeles, California and [2]JD Wheat Veterinary Orthopedic Research Laboratory, University of California, Davis, California

Corresponding Author
Kirk L. Wendelburg
4641 Colorado Blvd.
Los Angeles, CA 90039
wendelburg@asgvets.com

Submitted December 2014
Accepted May 2015

DOI:10.1111/vsu.12437

Objective: To determine if an interlocking bolt would limit subsidence of the biological fixation universal hip (BFX®) femoral stem under cyclic loading and enhance construct stiffness, yield, and failure properties.
Study Design: Ex vivo biomechanical study.
Animals: Cadaveric canine femora (10 pairs).
Methods: Paired femora implanted with a traditional stem or an interlocking stem (constructs) were cyclically loaded at walk, trot, and gallop loads while implant and bone motions were captured using kinematic markers and high-speed video. Constructs were then loaded to failure to evaluate failure mechanical properties.
Results: Implant subsidence was greater ($P = .037$) for the traditional implant (4.19 mm) than the interlocking implant (0.78 mm) only after gallop cyclic loading, and cumulatively after walk, trot, and gallop cyclic loads (5.20 mm vs. 1.28 mm, $P = .038$). Yield and failure loads were greater ($P = .029$ and .002, respectively) for the interlocking stem construct (1155 N and 2337 N) than the traditional stem construct (816 N and 1405 N). Version angle change after cyclic loading was greater ($P = .020$) for the traditional implant (3.89 degrees) than for the interlocking implant (0.16 degrees), whereas stem varus displacement at failure was greater ($P = .008$) for the interlocking implant (1.5 degrees) than the traditional implant (0.17 degrees).
Conclusion: Addition of a stabilizing bolt enhanced construct stability and limited subsidence of a BFX® femoral stem. Use of the interlocking implant may decrease postoperative subsidence. However, in vivo effects of the interlocking bolt on osseointegration, bone remodeling, and stress shielding are unknown.

Total hip arthroplasty (THA) is used commonly in the treatment of coxofemoral osteoarthritis to increase joint function and comfort in dogs.[1–3] Initially, in veterinary patients, THA stems were cemented in the femur with polymethyl methacrylate (PMMA). Although cemented THA is associated with overall high success, aseptic loosening has been reported in up to 7.2% of clinical cases[4–6] and up to 63% of cases may be affected based on postmortem examination.[7] Cementless THA systems were developed, in part, to overcome the complications associated with use of PMMA, including aseptic loosening, extraosseous cement granuloma formation, and particulate disease.[8–10]

Cementless THA stems must achieve short and long term stability within the femur. Uncemented stems, such as the biological fixation universal hip (BFX®) stem (BioMedtrix™, Biomedtrix, Boonton, NJ), rely on press-fit within the femoral canal for short term stability and osseointegration into the porous metal surface of the femoral component for long term stability.[9–11] Clinical reports of dogs with cementless THA did not identify failure of osseointegration and long term stability as important complicating factors.[3,9] However, press-fit implantation of a porous-coated stem in the femur results in a relatively small surface area of initial osseous contact,[12] and the bone ingrowth process is limited.[13] Further, micromotion is present between the implant and bone bed.[11,14] Micromotion as little as 100–500 μm is sufficient to inhibit bone ingrowth and leads to formation of a fibrous membrane and a mechanically unstable implant.[15–17] Reported clinical complications of cementless THA include fracture of the femoral diaphysis and greater trochanter (2–13.1% of cases),[1,18,19] intraoperative femoral fissuring (3.6–5.4%),[18,19] coxofemoral luxation (3–13.5%),[1,3,9,19] and stem migration (8.1%).[19]

Subsidence may be an early consequence of inadequate initial stability and inability to restrict weight bearing of the affected limb in the immediate perioperative period in dogs.[20] The importance of implant subsidence may be underestimated. In vivo reports evaluating subsidence of cementless stems are

Presented at the Veterinary Orthopedic Society Conference, Sun Valley, Idaho, March 2015.

scarce with stem subsidence of only 1–2.2 mm reported.[3,9] Subsidence is difficult to measure in vivo, although predictive factors for subsidence include low canal flare index (CFI) and low percentage of femoral canal fill (CF).[20,21] However, the effects of subsidence may be embedded in other clinical complications. Subsidence and femoral fractures share common risk factors and both occur early in the postoperative period, before osseointegration is likely to be substantive.[18,20,22] Subsided implants may contribute to the development of femoral fracture and coxofemoral luxation because of altered range of motion, particularly in abduction, change in femoral stem version angle, and increased lateral translation as a result of decreased gluteal muscle pull.[23] Prevention of subsidence could, therefore, reduce the incidence of THA-associated fractures and luxations. Subsidence may be limited by accurate preparation of the femur, optimal stem positioning, and implantation of an appropriate sized stem. The anatomic shape of a stem also contributes to the initial stability by maximizing CF.[20]

The BFX® system has been widely used since 2003 with >13,500 implantations worldwide to date.[24] However, femoral fracture associated with the BFX® hip replacement system has been reported to occur at an incidence of up to 13.1% and dogs of older age and lower CFI have been at higher risk of developing fracture.[18] Most fractures observed with the BFX® system propagate from the level of the femoral head and neck ostectomy, indicating that expansion of the femoral cortex by an acutely subsiding implant may be the underlying mechanism. Consequently, subsidence is likely to contribute to the development of femoral fracture, and prevention of subsidence could reduce the incidence of THA-associated fractures.

We hypothesized that modification of the traditional BFX® femoral stem implant by addition of a lateral interlocking bolt would increase stem initial stability that would prevent implant subsidence and increase resistance to femoral fracture. Our goals were to compare implant motion and failure mechanical properties between femora implanted with the traditional BFX® implant and femora implanted with a BFX® implant modified to incorporate an interlocking bolt.

MATERIALS AND METHODS

Specimen Collection

Ten paired femora were harvested from skeletally mature dogs euthanatized for reasons unrelated to this study (37.6 ± 9.6 kg, 9.6 ± 2.3 years old, mean ± SD). Written owner consent was obtained before euthanasia. All soft tissues were removed. Mediolateral and caudocranial oblique (Cd15M-CrLO) digital radiographs (72kVp, 3.6 mAs, TruDR™, Sound Technologies Medical Systems Inc, Carlsbad, CA) were taken with a 1 inch calibration marker to ensure bone normalcy distal to the femoral head and for implant sizing. Bones were wrapped in 0.9% NaCl-soaked laparotomy sponges, placed in sealed freezer bags, and stored at −20°C until implantation and testing. All radiographic measurements were performed by a single investigator (YB) using digital orthopedic planning software (VetPACS OrthoPlanner 2006, Sound Technologies).

Surgical Implants

For each pair of femora, 1 bone was implanted with a size 7, 8, or 9 Titanium BFX® femoral stem and the contralateral bone was implanted with the same sized, but interlocking, BFX® stem (Fig 1). Interlocking stem modifications were a 1.6 mm diameter hole through the center of the neck that was continuous with a 4.5 mm diameter threaded hole passing

Figure 1 Orthogonal views of a size 7 interlocking biological fixation universal hip (BFX®) stem with 16 mm interlocking bolt (left) and traditional BFX® stem (right).

Veterinary Surgery 45 (2016) 155–164 © 2016 The Authors. Veterinary Surgery published by Wiley Periodicals, Inc., on behalf of The American College of Veterinary Surgeons.

through the lateral aspect of the stem. Stabilizing 4.44 mm diameter interlocking titanium bolts measuring 12–18 mm in length were used with each interlocking implant. Additional design features of the stabilizing bolt included a threaded tip to engage the stem and direct the bolt into position and an adjacent tapered area to allow interlock into the neck of the prosthesis. A +0, 17 mm diameter prosthetic head was used for mechanical testing of all specimens. All implants used were manufactured by BioMedtrix.

Surgical Technique and Instrumentation

After overnight thawing at 4°C, implantation of femoral stems was performed according to manufacturer guidelines by a single surgeon (KLW) experienced with the implantation technique. Online randomization software (Urbaniak, G.C., & Plous, S, 2013 Research Randomizer, Version 4.0, https://www.randomizer.org/) was used to select which bone within a pair would be implanted with the interlocking BFX® stem, and the contralateral femur was implanted with a traditional BFX® stem of the same size. Femoral stem size was determined by radiographic template measurements. The largest stem size with the goal of filling the confines of the endosteal margins of the femoral metaphysis and diaphysis in both the mediolateral and craniocaudal projections was selected. The stem was seated at a level that reconstructed natural anatomy, guided by overlapping of the prosthetic femoral head on the natural head of the femur. Once stem size was determined for an individual bone and ordered from the manufacturer, authors were committed to its use and modifications at the time of implantation could not be performed. Standard recognized technique and instrumentation for BFX® were used for implantation of all femoral stems.[25]

After press-fit of the interlocking BFX® stem in the femur, a 1.6 mm-diameter hole was drilled (Smart Driver, Micro-Aire Surgical Instruments, Charlottesville, VA) through the lateral femoral cortex using the hole in the prosthesis neck as a drill guide. A 1.57 mm trocar tipped, smooth K-wire (IMEX Veterinary Inc, Longview, TX) was placed in the hole through the prosthesis neck and femoral cortex. The femoral cortical hole was enlarged to 4.5 mm diameter using a 4.5 mm cannulated drill bit (DePuy Synthes, West Chester, PA) over the K-wire in retrograde fashion (Fig 2). The K-wire was removed and a 4.5 mm drill bit (DePuy Synthes) mounted on a hand chuck (IMEX Veterinary Inc.) was used in a similar direction to complete the preparation of the osseous bed by removing a small amount of cancellous bone adjacent to the implant, taking care not to damage it. Bone debris in the cortical hole was removed by injection of 10 mL of 0.9% NaCl using a 12 mL syringe and 18 g hypodermic needle. A depth gauge (DePuy Synthes) was used to ensure that interlocking bolt length would be sufficient for the bolt to protrude beyond the lateral aspect of the created cortical hole once securely locked into place. Because availability of bolts was limited in this study, some of the bolts used were longer than needed. The bolt was inserted through the femoral cortex into the prosthesis and manually locked into place using a small (2.38 mm) hexagonal screwdriver (DePuy Synthes). The stem was mildly impacted to ensure the initial press-fit was maintained.

Figure 2 Surgical technique for placement of the interlocking stem's bolt. A 4.5 mm cannulated drill bit was used to drill the proximolateral aspect of the femoral cortex over a 1.57 mm diameter K-wire preplaced through the neck of the prosthetic.

Radiographs were repeated to verify femoral integrity and adequacy of implant positioning (Fig 3). Implant version angle was measured as reported by Bausman et al.[26] Measurements of craniocaudal canal fill (CF_{CC}) and mediolateral canal fill (CF_{ML}) were performed as reported by Lascelles et al.[3] Implanted femora were rewrapped in 0.9% NaCl-soaked laparotomy sponges and kept at 4°C for transfer to the testing facility.

Specimen Preparation

To secure the femur to the mechanical testing system, the distal 40% of the femur was transfixed with 2 diagonal trocar tipped, 2.38 mm diameter K-wires (IMEX Veterinary Inc.) and embedded in PMMA (Coe Tray Plastic, GC America Inc, Alsip, IL), which was allowed to set for at least 20 minutes before testing. A PMMA concave cast, congruent with the

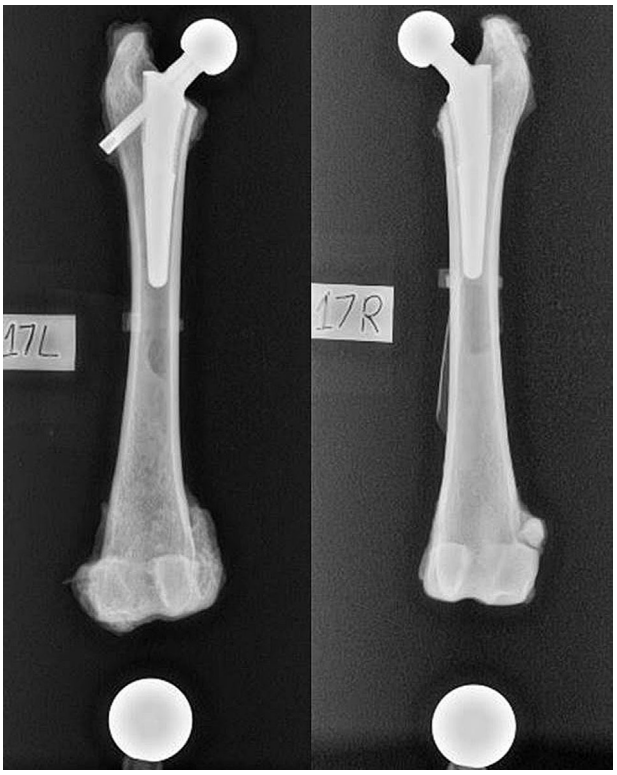

Figure 3 Postimplantation radiographs (Cd15M-CrLO) of femora with a size 7 interlocking biological fixation universal hip (BFX®) stem (left) and traditional BFX® stem (right).

Figure 4 Interlocking biological fixation universal hip (BFX®) stem construct preparation and positioning in the materials testing machine. Four kinematic painted markers were used: proximal femoral on the cranial aspect of the cortex, at a distance 20% of the bone's length from the proximal aspect of the greater trochanter; distal femoral at a 1 cm distance distal to the proximal femoral marker; head of the prosthesis; and neck of the prosthesis.

prosthetic femoral head, was used to transfer load to the femoral prosthesis.

Kinematic markers were painted (Liquitex, Piscataway, NJ) on the cranial surface of the head and neck of the implant and the femur (Fig 4). Markers allowed 3-dimensional (3D) tracking of implant motion (subsidence, varus, and version angles) using 2 high-speed video cameras (Fastcam PCI, Photron, San Diego, CA). The mechanical testing field was calibrated using an 8 marker cubic frame with known marker spatial relations.

Specimen constructs were mounted to the loading frame of a servohydraulic material testing machine (Model 809, MTS System Cooperation, Eden Prairie, MN) with the long axis of the femur placed parallel to the direction of loading (Fig 4). Load was applied to the prosthetic femoral head in a direction parallel to the longitudinal axis of the femur. Constructs were first loaded nondestructively, cyclically using a sinusoidal waveform at a frequency of 2 Hz at simulated walk (1200 cycles), trot (600 cycles), and gallop (600 cycles) loads (10–40%, 10–75%, and 10–155% of cadaveric body weight, respectively).[27–31] A 10% of cadaveric body weight preload was applied to comply with previously reported tests.[11,14,20] Kinematic data were acquired at 128 Hz. Specimens were completely unloaded at the end of each set of cycles to allow quantification of implant migration. After cyclic loading, constructs were loaded to failure in a single axial load cycle at a rate of 500 N/s. Load and construct displacement data were acquired at 128 Hz during the test. Digital photographs before and after failure were taken for documentation and to aid in failure mode characterization.

Data Processing and Reduction

Cyclic Data. Motion analysis software (Vicon Motus 9.1, CONTEMPLAS GmbH, Kempten, Germany) was used to digitize and calculate prosthesis migration relative to the bone from video images calibrated to 3D space. Cyclic load subsidence that occurred during the walk, trot, and gallop cycles, and cumulatively, was defined as the axial displacement of the prosthetic neck marker relative to the proximal femoral marker and was measured after unloading of the construct. Changes in prosthesis angular positions (cyclic version and varus angulation) were also calculated for the same interval and with the constructs fully unloaded as well. Variations in stem craniocaudal angles were not measured because of insufficient out-of-plane camera resolution.

Veterinary Surgery 45 (2016) 155–164 © 2016 The Authors. Veterinary Surgery published by Wiley Periodicals, Inc., on behalf of The American College of Veterinary Surgeons.

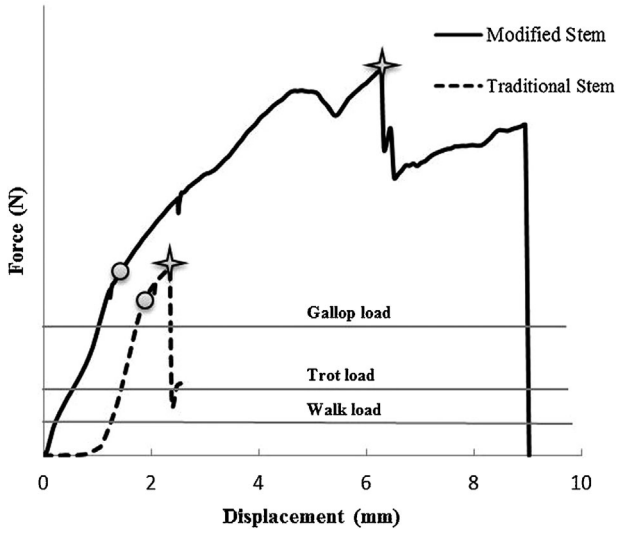

Figure 5 Representative force–displacement curves of paired femora. Failure (✦) and yield (◯) points are noted. Physiologic walk, trot, and gallop loads are marked for reference.

Failure Test Data. Force–displacement curves (Fig 5) were generated for failure data of each construct using custom software (Matlab, version 7.10, The Mathworks, Natick, MA) and used to quantify the following structural construct properties: stiffness (slope of the linear region of the force–displacement curve), yield (initiation of curve nonlinearity), and failure (point of maximum load before the construct no longer sustained load). Loads and implant displacements were determined from the respective yield and failure points. Yield and failure energies were calculated as the areas under the force–displacement curves to the respective points. Axial (subsidence) and angular (version and varus angles) stem displacements were also determined at the yield and failure points. Stem displacements were measured in a similar fashion to cyclic load subsidence and cyclic angular displacement but with the construct remaining loaded from testing initiation to reaching failure level. Failure patterns were determined by visual examination; mode of failure was simply categorized as bone failure versus implant failure.

Statistical Analysis

For cyclic testing, the effect of implant type (traditional BFX® vs. interlocking BFX® implants) and cyclic load level (40%, 75%, 155% body weight) on femoral stem migration (cyclic load subsidence and angular displacements) was assessed using paired *t*-tests. For failure testing, the effect of implant type (traditional vs. interlocking BFX® implant) on structural variables (construct stiffness, displacements, loads, and energies at yield and failure points) and on stem subsidence and angular variations was assessed using paired *t*-tests. Level of statistical significance for all tests was $P < .05$.

RESULTS

Specimen Preparation and Implants

Study femora accommodated implants of size 7 (5 pairs), 8 (1), and 9 (4). The only complication encountered during implantation was initial inability engaging the interlocking bolt into the stem of 1 femur because of a misaligned guide K-wire. Slight enlargement of the cortical hole resulted in successful bolt placement.

A mild periosteal reaction was present on the cranial surface of the proximal metaphysis of 1 femur implanted with a traditional BFX® stem. A mild decrease in cortical bone density was apparent on high resolution radiographs taken after mechanical testing. However, specimen failure did not occur through the affected region and mechanical properties and failure mode were similar to those of the other traditional constructs tested. Therefore, the data obtained from this construct were not excluded from the results.

No structural femoral complications, such as fissure lines resulting from stem implantation, were apparent on postimplantation radiographs (Fig 3). Although implant positioning was judged adequate in all specimens, stem under-sizing was noted in 6/20 (30%) constructs. No difference in mean stem anteversion angle ($P = .67$) was measured between interlocking BFX® implant constructs (21.3 ± 8.9 degrees) and traditional BFX® implant constructs (22.1 ± 7.5 degrees). No differences in craniocaudal and mediolateral CF ($P = .462$ and .537, respectively) were apparent between the interlocking BFX® implant (CF_{ML} 0.649 ± 0.051; CF_{CC} 0.595 ± 0.068)

Table 1 Stem Subsidence (Mean ± SD) for 10 Pairs of Traditional and Interlocking BFX® Implants After Cyclic Loading

	Traditional BFX® Stem	Interlocking BFX® Stem	*P*-Value
Subsidence (mm)			
Walk	0.23 ± 0.29	0.15 ± 0.27	.26
Trot	0.79 ± 1.21	0.35 ± 0.41	.28
Gallop	4.19 ± 4.51*	0.78 ± 0.67*	.04
Overall	5.20 ± 5.10*	1.28 ± 1.05*	.04
Version angle (degrees)			
Walk	1.33 ± 1.39	0.45 ± 1.09	.20
Trot	1.15 ± 2.06	−0.06 ± 1.01	.09
Gallop	1.41 ± 2.78	−0.23 ± 1.24	.09
Overall	3.89 ± 4.39*	0.16 ± 2.19*	.02
Varus angle (degrees)			
Walk	0.72 ± 0.74	0.81 ± 1.27	.80
Trot	0.57 ± 0.92	0.97 ± 0.83	.30
Gallop	0.95 ± 1.83	0.42 ± 1.12	.28
Overall	2.24 ± 2.99	2.20 ± 2.19	.97

BFX®, biological fixation universal hip.
*Indicates values that are significantly different. For each loading set of cycles (walk, trot, and gallop), values represent the change in subsidence or angular stem position that occurred during that set of cycles alone, while overall represents cumulative change throughout the entire cyclic phase of loading.

and the traditional BFX® implant (CF_{ML} 0.643 ± 0.049; CF_{CC} 0.584 ± 0.086).

Subsidence

Both the traditional and interlocking implants subsided after higher magnitudes of cyclic loading (Table 1). Minimal stem subsidence was measured after cyclic loading at walk and trot loads. However, the traditional BFX® implant subsided on average 4–5 mm after cyclic loading corresponding to gallop, which was significantly higher than the subsidence observed with the interlocking BFX® implant (1–2 mm). Axial stem displacement was not statistically different between implants during loading to failure (Table 2).

Angular Implant Motion

Version angle displacement was most pronounced after cyclic loading. The traditional implant had significantly higher anteversion change (3.89 ± 4.39 degrees) than the interlocking implant (0.16 ± 2.19 degrees; Table 1). Variation in varus angle between implants was only statistically significant at failure (Table 2) with the interlocking implant having greater varus angulation than the traditional stem.

Failure Properties

Yield and failure loads were 41 and 66% greater for interlocking implant constructs compared to traditional implant constructs (Table 2). Although preyield stiffness was higher for the traditional implant construct, post-yield stiffness was higher for the interlocking implant construct but neither difference reached statistical significance.

Failure Mode

All traditional implant constructs failed by developing a fissure or a long oblique fracture that propagated distally from the medial aspect of the femoral osteotomy site (familiarly known as the calcar). In all interlocking BFX® constructs, proximal bending of the bolt was first noted, followed by the bolt cutting through the lateral femoral cortex as a result of stem subsidence and subsequent fracture developing through the medial calcar. In 4 of the interlocking stems, the bolt completely broke.

DISCUSSION

Subsidence of THA femoral prostheses in cadaveric femora loaded ex vivo under physiologic cyclic loads and construct failure properties were compared between femora implanted with a traditional BFX® or interlocking BFX® femoral prosthesis. Ex vivo results supported the hypothesis that addition of a lateral interlocking bolt to the stem's design is likely to decrease subsidence and increase construct stability. Interlocking stems subsided less than traditional stems during cyclic loading and interlocking stem constructs had higher yield and failure loads than traditional stem constructs. Traditional stems had greater version angular change after cyclic loading, whereas interlocking stems had greater varus displacement when loaded to failure.

Table 2 Construct Yield and Failure Properties, and Corresponding Stem Displacements (Mean ± SD) for 10 Pairs of Traditional and Interlocking BFX® Implanted Femora After a Single Cycle of Axial Loading to Failure

	Traditional BFX® Stem	Interlocking BFX® Stem	*P*-Value
Yield			
Construct			
Stiffness (N/mm)	1,420 ± 298	1,178 ± 376	.07
Load (N)	817 ± 237¥	1,155 ± 370¥	.03
Displacement (mm)†	1.76 ± 1.02	1.82 ± 0.97	.73
Energy (N × mm)	356 ± 194	988 ± 1,118	.13
Stem displacement			
Axial (mm)*	0.23 ± 0.06	0.64 ± 0.70	.10
Varus angle (degrees)	0.33 ± 0.39	0.65 ± 0.51	.07
Version angle (degrees)‡	−0.10 ± 4.37	−3.48 ± 4.41	.36
Failure			
Construct			
Post-yield stiffness (N/mm)	236 ± 151	279 ± 177	.58
Load (N)	1,405 ± 752¥	2,337 ± 782¥	<.01
Displacement (mm)†	4.60 ± 3.26	6.29 ± 1.81	.13
Energy (N × mm)	4,198 ± 6,047	9,579 ± 6,076	.06
Stem displacement			
Axial (mm)*	3.49 ± 3.81	5.72 ± 4.03	.20
Varus angle (degrees)	0.17 ± 0.50¥	1.50 ± 0.97¥	.01
Version angle (degrees)‡	−2.73 ± 3.56	−3.79 ± 10.07	.86

*Axial stem displacement reflects the distance from the head marker to the proximal femoral marker.
†Construct displacement reflects testing machine platform displacement relative to the actuator.
‡Negative version angle value represents stem retroversion.
¥Indicates values that are significantly different.

Veterinary Surgery 45 (2016) 155–164 © 2016 The Authors. Veterinary Surgery published by Wiley Periodicals, Inc., on behalf of The American College of Veterinary Surgeons.

Risk factors for periprosthetic fracture include CF, CFI, implant fit, and dog age.[18] By using paired femora, we were able to limit bias because of differences in dog age and femoral CFI. Although CF was found to be insignificantly different between groups, implant fit (congruence) is more difficult to measure and was not evaluated. Except for a single pair, bone quality was assumed to be similar between paired femora, based on pre- and postimplantation radiograph evaluations as well as visual inspection of all bones. As a similar loading protocol was used for all paired constructs, the major factor likely to be accountable for differences in subsidence between groups is implant design.

The ex vivo cyclic testing protocol was developed to maximize clinical relevance while also complying with methods used in previous reports. Cyclic loading of an implant is related to the number of steps a dog takes after implantation and load magnitude with each step. Both load magnitude and step frequency are affected by gait and individual factors including dog size, age, and degree of discomfort as well as owner compliance following recommended instructions for strict activity restriction in the immediate perioperative period. A dog being walked 5–10 minutes 4 times daily will step on an individual limb ~1,500–3,000 times/day.[32] Because dogs undergoing THA are likely to be activity-restricted in the weeks after surgery, a 1,200 walk cycle protocol was used. Fewer cycles (600) of loading were used for trot and gallop loads because these activities would be unexpected events in the postoperative period and as a bone-implant micromotion steady state was observed after 600 cycles of loading of a cementless hip prosthesis in vitro.[14] Constructs were subjected to greater forces than anticipated during routine recovery to allow detection of the protective effect of the interlocking bolt. The ex vivo construct cyclic loading frequency (2 Hz) was greater than the mean limb stride frequency at a walk (1.24 strides/s).[33] Although bone is a viscoelastic material and thus would be stiffer and stronger at faster walk load rates, the observed differences between implant constructs would likely hold for walk, trot, and gallop loading rates.

The axial load protocol used in our study resulted in a similar fracture configuration to that observed in naturally occurring fractures. Longitudinal fissure lines or long oblique fractures propagating from the femoral ostectomy along the medial cortex of the bone were observed in our study. Similarly, 10/11 nontraumatic femoral fractures propagated obliquely from the femoral ostectomy within 23 days after surgery in dogs with a cementless THA.[18] In our study, the interlocking implant bolt also bent proximally and cut through the distal rim of the cortical hole at the lateral cortex to allow continued axial displacement of the implant as the ex vivo load continued to increase beyond physiologic levels. However, the direction and magnitude of the forces on the canine hip remain largely unknown. Although axial loading is common in in vitro studies,[20,21,34,35] combined axial and torsional loading is more likely to occur in vivo and was used more recently[36] in an attempt to simulate the long oblique or spiral fracture configuration observed in dogs with the Zurich cementless prosthesis (Kyon Inc, Zurich, Switzerland). The Zurich system may behave similar to an interlocking nail with shear forces originating from the locking bolt holes causing fissure propagation in torsion failure. In contrast, when a press-fit stem such as the traditional BFX® stem used in our study is axially loaded, the ability of the bone to resist hoop stresses predominately dictates stability.[36] The interlocking BFX® implant used in our study is thought to share properties of both of the above-mentioned implants; it relies on hoop stress for initial stability secondary to being press-fit into the femur, while the interlocking bolt may lead to shearing forces during torsion. As some degree of torsion is likely to be part of canine hip loading, bolt presence may predispose to torsional failure. The nature of failure fractures observed in our study is consistent with the concept that stem subsidence contributes to fracture development.

Initial stability of the interlocking prosthesis is primarily dependent on press-fit and is augmented by addition of the interlocking bolt. Careful surgical technique must be employed to ensure press-fit of the stem is not lost during bolt placement. Loss of press-fit may occur when difficulty placing the interlocking bolt is encountered (single construct in our study) as the increasing force applied to the bolt (directed 45° to the long axis of the bone) will have a distoproximal axial component that may dislodge the stem. In cases in which press-fit is lost, initial stem stability will be dependent on the integrity of the stabilizing bolt alone and may be inadequate. Addition of an alignment pin to the interlocking bolt design is being developed by the manufacturer to allow easier bolt placement and avoid press-fit interruption. The effect of the interlocking bolt on press-fit of the stem was not evaluated in our study. The cortical hole at the lateral femoral metaphysis may decrease the bone's ability to resist hoop stresses and result in decreased initial press-fit. In addition, the bolt may act as a stress riser at the bolt-bone interface leading to failure at the lateral cortex. An ex vivo study evaluating bolt location of an interlocking nail in the canine femur reported that metaphyseal bolts were able to sustain higher axial loads and that their constructs survived torsional loading, compared to diaphyseal bolts that failed under lower axial loads and 9/10 constructs failed under torsion.[37] No evidence for failure involving the bolt hole was noted in our study.

Placement of a hole through the body and neck of the interlocking stem may weaken the prosthesis. Computerized finite element analysis of the interlocking stem and bolt did not reveal any points of weakness but mechanical testing of the interlocking prosthesis has not yet been performed. Evidence for implant failure beyond breaking of the interlocking bolt in 4 constructs was not apparent in our study.

Long term effects of interlocking bolt addition remain unknown. The bolt may affect osseointegration and bone remodeling because of altered force distribution at the implant-bone interface and load concentration at the bolt-bone interface. Although implant-bone micromotion was not measured in our study, increased interlocking stem stability may limit micromotion and, therefore, facilitate earlier or stronger osseointegration. Reports of either canine or human proximal interlocking THA stem were not found in the literature. However, evaluation of mid term outcomes with use

of a human cementless distal interlocking hip revision stem reported no significant stress shielding, osteolysis, or radiographic loosening and all patients showed radiological evidence of implant osseointegration.[38] Clinical evaluation of the interlocking stem with long term followup is necessary to evaluate long term consequences of bolt addition.

Subsidence was less for the interlocking stem than the traditional stem, with differences between stems reaching statistical significance after gallop loads. Although stem axial displacement at yield and failure did not differ between implants, subsidence had already occurred in all constructs before initiation of the single cycle to failure test. A stronger press-fit of the traditional stem was likely achieved because of higher level of subsidence caused during cyclic loading. Although the interlocking bolt allowed minimal subsidence, under supraphysiologic loads applied during the failure tests, the bolt either slid through the cortical hole, yielded by bending, and/or failed by breaking, and cut through the lateral femoral cortex, all of which allowed greater axial deformation of the interlocking implant construct in comparison to the traditional implant construct. Furthermore, the interlocking implant yielded and ultimately failed under significantly greater loads than the traditional stem with no difference in construct displacement or stem axial deformation, therefore displaying greater stability. However, ex vivo yield and failure loads were greater than the magnitude of the walk, trot, and gallop loads for both traditional and interlocking constructs.

The guide K-wire used for bolt placement has a smaller diameter (1.57 mm) than the inner diameter of the cannulated drill bit (2.38 mm). A better fit between guide-wire and cannulated drill bit will eliminate relative motion or rocking of the drill bit over the wire and the potential creation of a cortical hole larger in diameter than the 4.44 mm interlocking bolt. Indeed, the creation of a cortical defect between the bolt and the distal extent of the hole can also contribute to the development of subsidence or construct deformation or both. BioMedtrix is currently developing a more suitable cannulated drill bit to resolve this issue.

Other factors, in addition to cortical hole/bolt diameter disparity, could have contributed to the trend for a lower initial stiffness during the failure test of the interlocking implant construct compared to the traditional implant construct. Bolt deformation (bending), sliding through the cortical hole, or fissuring the lateral femoral cortex would have contributed to interlocking implant construct deformation and lower stiffness. Implant bone interface frictional forces and conversion of axial forces to hoop stresses could have been greater for the traditional implant construct because of increased contact area of the more highly subsided traditional implant. The interlocking stem's bone contact area would have been lower at the initiation of the failure test, allowing greater implant displacement relative to the bone, resulting in a relatively lower interlocking implant construct stiffness.

Both implant designs reached the yield and failure points under higher loads than those expected to be generated during walk, trot, or gallop, making it unlikely for either of the 2 designs to fail catastrophically in the early postoperative period. On the other hand, accidental lapse in activity restriction may lead to much higher peak vertical forces. Vertical pelvic limb forces measured during agility activity were >20 N/kg body weight for running, >30 N/kg body weight for landing from hurdle jump, and nearly 40 N/kg body weight for jumping from a long jump.[39] For the average cadaveric body weight in our study, a 37 kg dog landing from a long jump will load the pelvic limb in excess of 1,400 N, which may lead to construct failure as it exceeds loads to yield and even failure of the traditional implant (816 N and 1,405 N, respectively). Conversely, the higher loads to yield and failure of the interlocking implant (1,155 N and 2,337 N, respectively) may protect against catastrophic failure in such scenarios.

In our study, undersized stems may have led to overestimation of the protective value of the locking bolt because of low CF. Although the mean CF was insignificantly different between the traditional and interlocking implant groups, CF was lower than previously reported in a single clinical series[9] and surgical technique guidelines.[25] Although low CF is suggestive that undersized stems were used in our study, differences in stem design, cadaveric bone anatomy, CF measurement technique, and radiographic projections used for CF measurement may account, in part, for the lower CF measured in our study compared to previous reports. In addition, although low CF was identified as a risk factor for subsidence in several reports,[20,21,40] other publications did not support such an association.[9,19] Nonetheless, stem undersizing was identified in 30% of constructs based on subjective postimplantation radiographic assessment. Stem undersizing may have resulted from using computerized stem templates based on the previous and larger BFX® stem design and the limited availability of only size 7–9 stems from the manufacturer. Consequently, available cadaveric femora were matched to available stem sizes.

Craniocaudal angular deformation of the stems could not be evaluated in our study. High-speed video was used to capture and measure implant migration relative to the bone. Two video cameras were used in an attempt to capture 3D motion, and camera configuration proved to result in inadequate resolution for detection of craniocaudal angular changes. The importance of implant craniocaudal angular changes in our study is unknown. However, previous studies,[11,14] assessing initial stability of femoral stems, reported subsidence and version angle changes as being most pronounced, and both were adequately assessed in our study and were associated with significant differences between stem designs.

Perhaps, the most clinically relevant finding of our study, decreased stem subsidence of the interlocking BFX® implant under cyclic loading, may contribute to decreasing the risk of inadequate biologic fixation and perioperative fractures. However, followup clinical studies are required to confirm the importance of our findings. Indeed, the ex vivo conditions under which cadaveric bones are tested do not completely replicate in vivo loading (for example lack of torsional loading), nor do ex vivo studies account for bone modeling and remodeling changes that occur in vivo in response to altered loading environment and implant micromotion.

Veterinary Surgery 45 (2016) 155–164 © 2016 The Authors. Veterinary Surgery published by Wiley Periodicals, Inc., on behalf of The American College of Veterinary Surgeons.

In conclusion, our results show that addition of an interlocking bolt enhanced construct stability and limited subsidence of a BFX® femoral stem under the experimental conditions of our study. Although care must be taken when attempting to extrapolate results of an ex vivo study to live animals, the findings of our study indicate that use of the interlocking implant may decrease postoperative femoral fractures resulting from excessive subsidence. Further in vivo evaluation of the interlocking BFX® stem is warranted.

ACKNOWLEDGMENTS

The authors thank Chris Sidebotham and BioMedtrix for their professional advice and donation of the implants used in our study.

DISCLOSURE

Dr. Wendelburg has a US patent pending for the interlocking BFX® implant and may receive future royalties from BioMedtrix. All implants used in this study were donated by BioMedtrix. The authors declare no other conflicts of interest related to this study.

REFERENCES

1. DeYoung DJ, DeYoung BA, Aberman HA, et al: Implantation of an uncemented total hip prostheses, technique and initial results of 100 arthroplasties. *Vet Surg* 1992;21:168–177
2. Barden TD, Olivier NB, Blaiset MA, et al: Objective evaluation of total hip replacement in 127 dogs utilizing force plate analysis. *Vet Comp Orthop Traumatol* 2004;17:78–81
3. Lascelles BD, Freire M, Roe SC, et al: Evaluation of functional outcome after BFX® total hip replacement using a pressure sensitive walkway. *Vet Surg* 2010;39:71–77
4. Olmstead ML: Total hip replacement. *Vet Clin North Am Small Anim Pract* 1987;17:943–955
5. Edwards MR, Egger EL, Schwarz PD: Aseptic loosening of the femoral implant after cemented total hip arthroplasty in dogs: 11 cases in 10 dogs (1991–1995*)*. *J Am Vet Med Assoc* 1997;211:580–586
6. Ota J, Cook JL, Lewis DD, et al: Short-term aseptic loosening of the femoral component in canine total hip replacement: effects of cementing technique on cement mantle grade. *Vet Surg* 2005;34:345–352
7. Skurla CP, Pluhar GE, Frankel DJ, et al: Assessing the dog as a model for human total hip replacement. Analysis of 38 canine cemented femoral components retrieved at post-mortem. *J Bone Joint Surg Br* 2005;87:120–127
8. Bergh MS, Gilley RS, Shofer FS, et al: Complications and radiographic findings following cemented total hip replacement. *Vet Comp Orthop Traumatol* 2006;19:172–179
9. Marcellin-Little DJ, DeYoung BA, Doyens DH, et al: Canine uncemented porous-coated anatomic total hip arthroplasty: results of a long term prospective evaluation of 50 consecutive cases. *Vet Surg* 1999;28:10–20
10. Hummel DW, Lanz OI, Werre SR: Complications of cementless total hip replacement. *Vet Comp Orthop Traumatol* 2010;23:424–432
11. Schneider E, Kinast C, Eulenberger J, et al: A comparative study of the initial stability of cementless hip prostheses. *Clin Orthop Relat Res* 1989;248:200–209
12. Schimmel JW, Huiskes R: Primary fit of the Lord cementless total hip: a geometric study in cadavers. *Acta Orthop Scand* 1988;59:638–642
13. McKoy BE, An YH, Friedman RJ: Factors affecting the strength of the bone-implant interface, in An YH, Draughn RA (eds): *Mechanical testing of bone and the bone-implant interface*. Boca Raton, FL, CRC Press, 2000, pp 439–462
14. Schneider E, Eulenberger J, Steiner W, et al: Experimental method for the in vitro testing of the initial stability of cementless hip prostheses. *J Biomech* 1989;22:735–744
15. Jasty M, Bragdon C, Burke D, et al: In vivo skeletal responses to porous-surfaced implants subjected to small induced motions. *J Bone Joint Surg Am* 1997;79:707–714
16. Aspenberg P, Goodman S, Toksvig-Larsen S, et al: Intermittent micromotion inhibits bone ingrowth. *Acta Orthop Scand* 1992;63:141–145
17. Overgaard S, Lind M, Glerup H, et al: Porous-coated versus grit-blasted surface texture of hydroxyapatite-coated implants during controlled micromotion. *J Arthrop* 1998;13:449–458
18. Ganz SM, Jackson J, VanEnkevort B: Risk factors for femoral fracture after canine press-fit cementless total hip arthroplasty. *Vet Surg* 2010;39:688–695
19. Townsend KL, Kowaleski MP, Rajala-Shultz P, et al: Radiographic analysis of Biomedtrix cementless femoral stem implants as a predictor for subsidence. *Vet Surg* 2007;36: E26
20. Rashmir-Raven AM, DeYoung DJ, Abrams CF, et al: Subsidence of an uncemented canine femoral stem. *Vet Surg* 1992;21:327–331
21. Pernell RT, Gross RS, Milton JL, et al: Femoral strain distribution and subsidence after physiological loading of a cementless canine femoral prosthesis: the effects of implant orientation, canal fill, and implant fit. *Vet Surg* 1994;23:503–518
22. DeYoung DJ, Schiller RA, DeYoung BA: Radiographic assessment of a canine uncemented porous-coated anatomic total hip prosthesis. *Vet Surg* 1993;22:473–481
23. Bartel DL, Dueland RT, Quentin JA: Biomechanical considerations in the design of a canine total hip prosthesis. *J Am Anim Hosp Assoc* 1975;11:553–559
24. BioMedtrix internal clinical follow-up report: cementless THR, April 2014
25. BioMedtrix universal canine hip system. Surgical technique for BFX® cementless and CFX® cemented implants, BioMedtrix, Boonton, New Jersey. Released August 28, 2007
26. Bausman JA, Wendelburg KL: Femoral prosthesis version angle calculation from a saggital plane radiographic projection of the femur. *Vet Surg* 2013;42:398–405
27. Budsberg SC, Verstraete MC, Soutas-Little RW: Force plate analysis of the walking gait in healthy dogs. *Am J Vet Res* 1987;48:915–918

28. Bockstahler BA, Skalicky M, Peham C, et al: Reliability of ground reaction forces measured on a treadmill system in healthy dogs. *Vet J* 2007;173:373–378

29. Bertram JE, Lee DV, Case HN, et al: Comparison of the trotting gaits of Labrador Retrievers and Greyhounds. *Am J Vet Res* 2000;61:832–838

30. Budsberg SC, Verstraete MC, Brown J, et al: Vertical loading rates in clinically normal dogs at a trot. *Am J Vet Res* 1995;56:1275–1280

31. Walter RM, Carrier DR: Ground forces applied by galloping dogs. *J Exp Biol* 2007;210:208–216

32. Aper RL, Litsky AS, Roe SC, et al: Effect of bone diameter and eccentric loading on fatigue life of cortical screws used with interlocking nails. *Am J Vet Res* 2003;64:569–573

33. Hottinger HA, DeCamp CE, Olivier NB, et al: Noninvasive kinematic analysis of the walk in healthy large breed dogs. *Am J Vet Res* 1996;57:381–388

34. Dosch M, Hayashi K, Garcia TC, et al: Biomechanical evaluation of the Helica femoral implant system using traditional and modified techniques. *Vet Surg* 2013; 42:867–876

35. McCulloch RS, Roe SC, Marcellin-Little DJ, et al: Resistance to subsidence of an uncemented femoral stem after cerclage wiring of a fissure. *Vet Surg* 2012;41:163–167

36. Pozzi A, Peck JN, Chao P, et al: Mechanical evaluation of adjunctive fixation for prevention of periprosthetic femur fracture with the Zurich cementless total hip prosthesis. *Vet Surg* 2013;42:529–534

37. Burns CG, Litsky AS, Allen MJ, et al: Influence of locking bolt location on the mechanical properties of an interlocking nail in the canine femur. *Vet Surg* 2011;40:522–530

38. Carrera L, Haddad S, Minguell J, et al: Mid-term outcomes and complications with cementless distal locking hip revision stem with hydroxyapatite coating for proximal bone defects and fractures. *J Arthrop* 2015;30:1035–1040

39. Pfau T, Garland de Rivaz A, Brighton S, et al: Kinetics of jump landing in agility dogs. *Vet J* 2011;190:278–283

40. Townsend KL, Kowaleski MP, Johnson KA: Initial stability and femoral strain pattern during axial loading of canine cementless femoral prostheses: effect of resection level and implant size. *Proceedings of the Veterinary Orthopedic Society*, Sun Valley, ID, March 2007